BILINGUAL PUBLISHING CO.
Pioneer of Global Academics Since 1984

Journal of Metallic Material Research
https://ojs.bilpublishing.com/index.php/jmmr

ARTICLE

Interpretation of Water Samples by Correspondence Analysis for Radioactive Elements in the Northern Coast of Oman Sea

Farshad Darabi-Golestan[1*] Mohamad Reza Zare[2]

1. Department of Mining and Metallurgical Engineering, Amirkabir University of Technology, Tehran, Iran
2. Department of Physics, Faculty of Sciences, University of Isfahan, Isfahan, 81746-73441, Iran

ARTICLE INFO

Article history
Received: 29 March 2022
Accepted: 24 April 2022
Published Online: 5 May 2022

Keywords:
Hormoz canyon
R-mood analysis
Correspondence analysis
Radioactive elements
Marine spot samples

ABSTRACT

Oman Sea is connecting belt between the Indian Ocean and Persian Gulf. Because it strategic and environmental aim, presence of natural radionuclide ^{226}Ra, ^{232}Th, ^{40}K and ^{137}Cs as man-made element is considered. Water samples were taken from 36 marine spots at the coastal strip from Hormoz canyon to Goatr seaport in the northern coast of Oman Sea. Correspondence analysis is used to identify variation and relationship between samples (Q-mood analysis) and variable (R-mood analysis) based on approximate χ^2 distances. Radioactive elements (^{226}Ra, ^{232}Th and ^{40}K), physical (temperature, pH, turbidity, conductivity, special density) and chemical (salinity, oxygen and chlorophyll) parameters of water for 36 samples handled by correspondence analysis, there are two outstanding result, 1) Radioactive elements show high correlation in factors by greater eigenvalue, and 2) some of the samples such as W13, W24 and rather W02, W05 and W12 show highest activity from Radioactive elements and also temperature and conductivity show nearest relation with them in many factors.

1. Introduction

The radionuclides are the source of natural radioactivity in earth [1,2]. Some effective dose of natural radioactivity received by human acts in the world. Large amounts of radionuclides have been released into the environment after the Fukushima and Chernobyl nuclear accidents [3]. The current research tries to create a reference value to future investigation. Therefore, the data can be basic values in the region, while the results always are comparable data in each. It was necessary to mention that this the same type of this research was published for many countries, such as Ireland, Egypt [4,5], India [6], China [7], America [8], Turkey [9] and Mexico [10]. According to the International Atomic Energy Agency (2003) [11], the standard systematic sampling was taken at the northern coastline of Oman Sea.

Water quality assessment studies, especially in coastal seas from natural radionuclides have been frequently conducted in many countries at the last years [12,13]. The

*Corresponding Author:
Farshad Darabi-Golestan,
Department of Mining and Metallurgical Engineering, Amirkabir University of Technology, Tehran, Iran;
Email: pooyan@aut.ac.ir

DOI: https://doi.org/10.30564/jmmr.v5i1.4571

variables and samples analysis were done by Correspondence Analysis (CA) according to covariance and distance parameters from R-mode and Q-mode analysis respectively [14-16]. Accordingly, indicator samples were adjusted in the spatial neighborhood of related variables [17]. Monitoring of the radioactivity for all radionuclides is the main environmental aim at each country. Besides these data could be considered as reference data to check the radioactivity changes during too many years. During this study, the interaction effect of conductivity, temperature, special density, salinity, chlorophyll, oxygen, turbidity and pH parameters against ^{226}Ra, ^{232}Th and ^{40}K radionuclides has been considered using multivariate analysis. Some of these parameters show best similarity to detect radionuclide concentrations.

2. Materials and Methods

The total number of 36 marine spot was designed in the northern coast of Oman Sea. The first related sample was taken from the Hormoz canyon and it continued by coastal strip to Goatr seaport. The sampling project was done in May 2011 and covered an area between 56° 30′ to 61° 30′ in longitude and 25° to 26° in latitude. Figure 1 shows the location of sampling spots, afterward the sample code and location of each sample represented in Table 1. A hand-held EXPLORANIUM spectrometer was applied to monitoring and detect the environmental changes [18,19]. By using the CTD system could record conductivity (MS/cm), temperature (°C), special density (gr/cm^3), salinity (PSU), chlorophyll (mgr/m^3), oxygen (PPM), turbidity (NTU) and pH of water. A suitable pump was used to suction about 100 liters of surface water from the Oman gulf. A container applied to minimize the absorption of activity. Accordingly, the pH of water solution decreases to 1.5 and High-Purity Germanium (HPGe) are used to detect of high-precision digital electronics of all parameters [6-20]. The portable HPGe detector positioned vertically inverse at center of the water sample [21,22]. All samples were taken from the nearest coastal strip and each spot designed which could probe possible polluting sources. All the statistic and multivariate analysis are done using Minitab 19.2020.1 (64-bit) and SPSS Statistics 17.

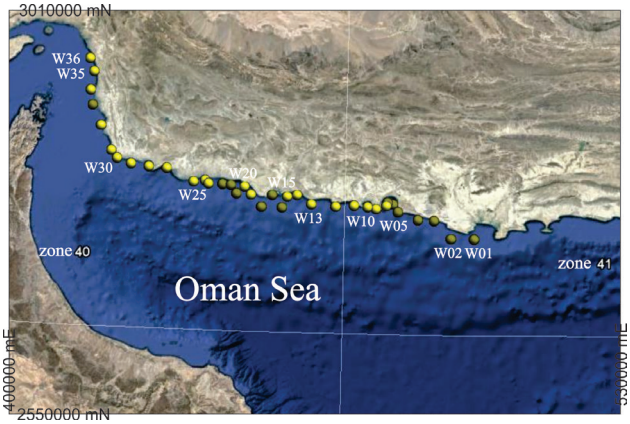

Figure 1. Locations map of the sampling spots consist of water samples

Table 1. The location of water samples in Oman Sea

Sample code	location	Sample code	location
W01	Chabahar Seaport (Pasabandar)	W19	Pi Bashk (Karti)
W02	Chabahar Seaport (Baris Bala)	W20	Pi Bashk (Lirdaf)
W03	Chabahar Seaport (Baris Bala)	W21	Pi Bashk (Sadich)
W04	Chabahar Seaport	W22	Pi Bashk (Sadich)
W05	Chabahar Seaport	W23	Pi Bashk (Kentaki)
W06	Chabahar Seaport (Konarak)	W24	Pi Bashk (Kentaki)
W07	Chabahar Seaport (Konarak)	W25	Pi Bashk (Kentaki)
W08	Chabahar Seaport (Konarak)	W26	Jask Seaport
W09	Chabahar Seaport (Konarak)	W27	Jask Seaport
W10	Chabahar Seaport (Konarak)	W28	Jask Seaport
W11	Chabahar Seaport (Gordim)	W29	Jask Seaport
W12	Pi Bashk (Tong Seaport)	W30	Jask Seaport
W13	Pi Bashk (Hoomadan)	W31	Jask Seaport
W14	Pi Bashk (Derak)	W32	Taherooi (Serich)
W15	Pi Bashk (Derak)	W33	Taherooi (Mashi)
W16	Pi Bashk (Derak)	W34	Taherooi (Mashi)
W17	Pi Bashk (Karti)	W35	Taherooi (Sirik Seaport)
W18	Pi Bashk (Karti)	W36	Gheshm

3. Results

3.1 Statistical Analysis

The minimum and maximum, mean and median, standard deviation, variance, values of ^{226}Ra, ^{232}Th and ^{40}K are showed in Table 2. The boxplot that displays the distribution of median confidence interval box, outlier symbols, median symbol and the minimum and maximum, mean for Ra, Th, and K (Figure 2).

3.2 Correspondence and K-means Analysis

Correspondence Analysis (CA) method is a useful method in order to geochemical classification of variables [23,24]. By application of this method could reduce high-dimensional data into subset of data which have low-dimension. These data could easily interpret and show effective and simple dimension. The subspaces reveal the main variances between variables [25-28]. R-mode and Q-mode are the two main branches of CA method [28,29]. The Q-mode (represented as sample-to-sample analysis) and R-mode (represented as element-to-element) are the two main results of the CA analysis. The results of R-mode and Q-mode matrix are combined as F-matrix while the distances are χ^2 distances between the respective modes [30,25]. Therefore, the CA could easily indicate the similarity or association between variables (R-mode, which represented by loadings or blue vectors in Figure 3) derived from data samples (Q-mode, which represented by scores or red symbols in Figure 3). The first (82% of Inertia) and second (9.6% of Inertia) CA factors with the highest eigenvalue are the stronger factors. The cumulative proportion of inertia for the first and second factor consists of 91.5% of total variation in the whole samples (Table 3). The symmetric with combination of the first and second factor is displayed in Figure 2. Both row and column principal coordinate overlaid in new dimensions. This method could ease difficulty between variables while there are not of primary interest in data (for columns and rows). Therefore, columns (variables) and rows (samples) plotted in new dimension.

Table 2. Descriptive statistics of water samples for ^{226}Ra, ^{232}Th and ^{40}K activity concentration.

	Variable	Minimum	Maximum	Mean	Median	St.Dev.	Variance
water sample (Bq/Lit)	^{226}Ra	2.19	2.82	2.4917	2.555	0.1794	0.0322
	^{232}Th	1.66	2.17	1.9031	1.885	0.1514	0.0229
	^{40}K	132.6	148.87	141.48	144.42	5.87	34.51

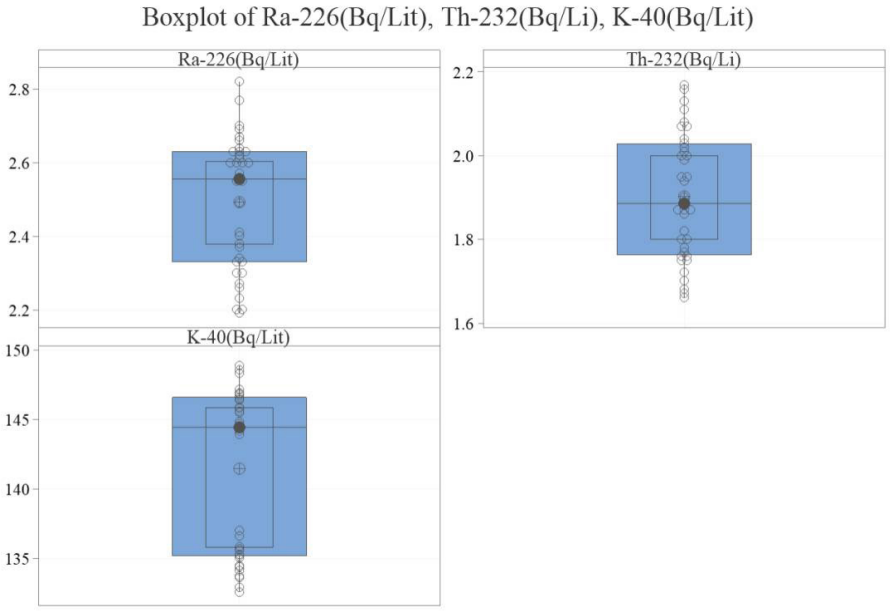

Figure 2. The boxplot of Ra, Th and K for water samples

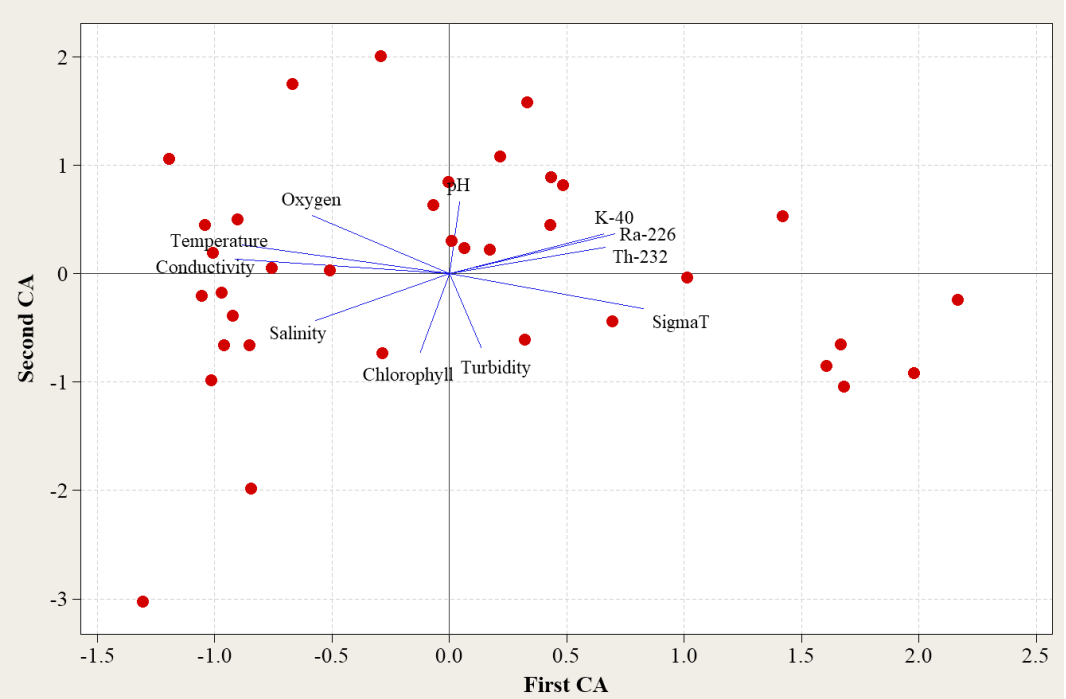

Figure 3. The 2-D symmetric plot from multivariate CA analysis for the first and second dimensions in the water samples.

The parameters and radionuclides are plotted within new dimension according to Euclidian distances between observations by covariance-based and distance-based analysis. *Symbols are the special dispersion pattern of sample in the new dimension that represent amount of concentration in samples.

Table 3. The Contingency table from CA analysis

Axis	Inertia	Proportion ratio	Cumulative
1	0.0094	0.8190	0.8190
2	0.0011	0.0961	0.9151
3	0.0007	0.0629	0.9780
4	0.0001	0.0125	0.9906

4. Discussion

A set of samples in a K-means cluster are more similar to each other according to some similarity or dissimilarity measures. Therefore, it was used and revealed that samples show different properties due to their parameters. All samples were categorized in 4 groups (Figure 4), while the first group (which have 13 observations) shows higher value for Ph, K, Ra, Th. The second and the third group have 7 and 8 samples, respectively. They are more important for temperature, conductivity, salinity. Parameters. The fourth group by 8 samples show higher turbidity and sigma-T. The first dimension of CA indicates maximum variance between ^{226}Ra, ^{232}Th and ^{40}K parameters and temperature, sigma-T, oxygen, conductivity. On the other hand, the second dimension of CA analysis indicates different Eigenvector for pH, turbidity, chlorophyll, and salinity parameters.

The sample numbers of W13, W18 and W24 are strongly, in which W12, W05 and W02 are moderately concentrated from ^{226}Ra, ^{232}Th and ^{40}K radionuclides (Figure 4). According to the Figure 2 it would have revealed that sample W13 and W18 (Eigenvalues distinguished by black circles, Figure 4) have been concentrated from ^{226}Ra, ^{232}Th and ^{40}K radionuclides (shown by blue eigenvectors, Figure 3), whereas, W26 and W03 show at least values. On the other hand, W26 and W35 sample numbers considered as the highest values of salinity and chlorophyll. All the water variation from radionuclides indicated by the 2D graphical representation of eigenvalues and eigenvectors (Figure 3), simultaneously in the correspondence (CA) and factor analysis combination. The sample numbers of W18, W34, W21, W08, W04, W13 and W24 can straighten this idea. Also, the second dimension of variation in CA indicates that turbidity, chlorophyll, and salinity have the minimum similarities with ^{226}Ra, ^{232}Th and ^{40}K radionuclides and it is indicated according to W26 and W35 samples. During this paper concluded that Sigma-T and pH considered as best indicator for radionuclides concentration. Higher concentrated values for salinity and conductivity may be originated from at least values for ^{226}Ra, ^{232}Th and ^{40}K radionuclides.

Activity concentrations of radionuclides of ^{40}K, ^{226}Ra and ^{232}Th were measured (Table 2) and results compared with international standard values and legal regulations (Table 4). Maximum activity concentration of ^{226}Ra and ^{40}K was measured respectively 2.82 Bq/Lit and 148.87 Bq/Lit in sample number 13 at Pi Bashk (Hoomadan). Accordingly, the maximum value of ^{232}Th was 2.17 Bq/Lit in sample number W34 at Taherooi (Mashi). The natural activity concentrations of radionuclides of ^{40}K, ^{226}Ra, and ^{232}Th have been estimated below the significant values in the world.

Table 4. The compression of concentrations of K, Ra and Th northern coast of Oman sea with international standard values and legal regulations

Country	^{40}K	^{232}Th	^{226}Ra	References
Nigeria	7.51±0.56	1.78±0.14	2.99±0.57	[31]
Earth's crust average	400	30	-	[32]
Albania (minimum-maximum)	266-675	13-40	13-23	[33]
India, East coast of Tamilnadu (CSS)	360.23	14.29	-	[34]
Saudi coastline, Gulf of Aqaba (CSS)	641.1	22.5	-	[35]
Greateraccra, Ghana (CSS)	29.78	108.6	-	[36]
Egypt red sea (Marine sediment)	330.70 ± 107	16.19 ± 8.68	-	[37]
Iran (Anzali wetland) (minimum-maximum)	371.8-652.28	17.57-45.84	13.83-38.37	[38]
Iran (northern coast of Oman Sea, CSS)	141.48	1.9031	2.4917	Present study

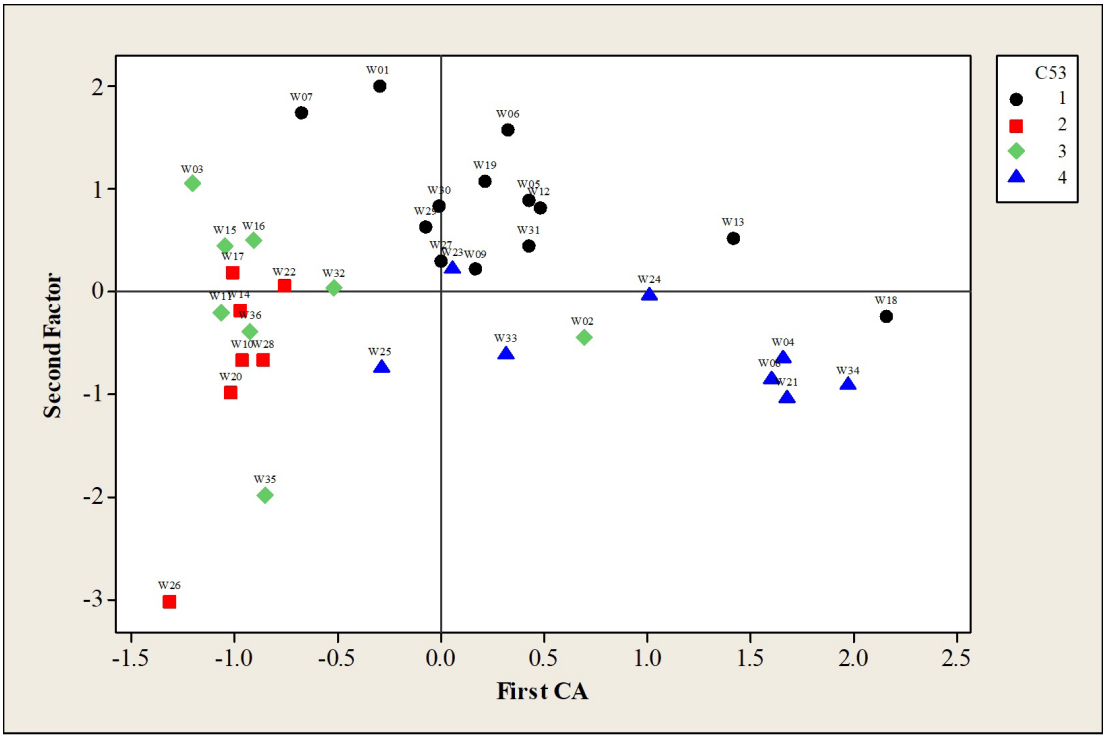

Figure 4. The graphical combination plot of CA and K-means clustering.

5. Conclusions

Correspondence analysis is applied to recognize water sample and analyzed variable (three radioactive element and eight physical and chemical properties of sample). In these surveys, variables of Ra, Th and K have different specification from conductivity, temperature, special density, salinity, chlorophyll, oxygen, turbidity and pH of water. Accordingly, these radionuclides have same behavior (with high eigenvalue) and correlated in stronger factors. Therefore, samples such as W13, W24, W18 (strongly) and W12, W05 and W02 (moderately) are concentrated from Th, Ra and K. By application of CA and factor multivariate analysis, the first dimension shows the conductivity, temperature, O_2 and salinity parameters have distinctly different from ^{226}Ra, ^{232}Th and ^{40}K according to covariance-based (R-mode) analysis. On the other hand, the second dimension indicates temperature, O_2, and conductivity and maybe pH have a high correlation with radionuclides. Finally, after analysis, the values of the ^{226}Ra, ^{235}U, ^{40}K, ^{232}Th, and ^{137}Cs concentrations in water samples were lower than that value of the world. Therefore, the data can be basic values in the region and accepted as a reference and comparable data in each time. During this paper concluded that Sigma-T and pH considered as best indicator for radionuclides concentration. Higher concentrated values for salinity and conductivity may be originated from at least values for ^{226}Ra, ^{232}Th and ^{40}K radionuclides. Regarding these parameters, all the data are below the significant values in the world but it suggested that Pi Bashk (Hoomadan) and Taherooi (Mashi) stations need to be studied in the future.

Conflict of Interest

There is no conflict of interest.

References

[1] Abdi, M., Faghihian, H., Mostajaboddavati, M., et al., 2006. Distribution of natural radionuclides and hot points in coasts of Hormozgan, Persian Gulf, Iran. Journal of Radioanalytical and Nuclear Chemistry. 270(2), 319-324.

[2] Alatise, O., Babalola, I., Olowofela, J., 2008. Distribution of some natural gamma-emitting radionuclides in the soils of the coastal areas of Nigeria. Journal of Environmental Radioactivity. 99(11), 1746-1749.

[3] Matisoff, G., Ketterer, M.E., Rosén, K., et al., 2011. Downward migration of Chernobyl-derived radionuclides in soils in Poland and Sweden. Applied Geochemistry. 26(1), 105-115.

[4] Harb, S., 2008. Natural radioactivity and external gamma radiation exposure at the coastal Red Sea in Egypt. Radiation Protection Dosimetry. 130(3), 376-384.

[5] Uosif, M., El-Taher, A., Abbady, A.G., 2008. Radiological significance of beach sand used for climatotherapy from Safaga, Egypt. Radiation Protection Dosimetry. 131(3), 331-339.

[6] Gouda, M., Hamzawy, A., Badawi, M., et al., 2016. Mathematical method to calculate full-energy peak efficiency of detectors based on transfer technique. Indian Journal of Physics. 90(2), 201-210.

[7] Xu, L., Liu, X., Sun, L., et al., 2010. Distribution of radionuclides in the guano sediments of Xisha Islands, South China Sea and its implication. Journal of Environmental Radioactivity. 101(5), 362-368.

[8] Myrick, T., Berven, B., Haywood, F., 1983. Determination of Concentrations of Selected Radionuclides in Surface Soil in the US. Health Physics. 45(3), 631-642.

[9] Kurnaz, A., Küçükömeroğlu, B., Keser, R., et al., 2007. Determination of radioactivity levels and hazards of soil and sediment samples in Fırtına Valley (Rize, Turkey). Applied Radiation and Isotopes. 65(11), 1281-1289.

[10] Mireles, F., Davila, J., Quirino, L., et al., 2003. Natural soil gamma radioactivity levels and resultant population dose in the cities of Zacatecas and Guadalupe, Zacatecas, Mexico. Health Physics. 84(3), 368-372.

[11] International Atomic Energy Agency, 2003. Collection and Preparation of Bottom Sediment Samples for Analysis of Radionuclides and Trace Elements. IAEA-TEC-DOC 1360, IAEA, Vienna (technical report).

[12] Yasmin, S., Barua, B.S., Kamal, M., et al., 2014. An Analysis for Distribution of Natural Radionuclides in Soil, Sand and Sediment of Potenga Sea Beach Area of Chittagong, Bangladesh. Journal of Environmental Protection. 5(17), 1553.

[13] Zare, M.R., Kamali, M., Kapourchali, M.F., et al., 2016. Investigation of ^{235}U, ^{226}Ra, ^{232}Th, ^{40}K, ^{137}Cs, and heavy metal concentrations in Anzali international wetland using high-resolution gamma-ray spectrometry and atomic absorption spectroscopy. Environmental Science and Pollution Research. 23(4), 3285-3299.

[14] Aggrawal, D., Bansal, G., Anand, A., et al., 2016. Types of Customers Surrounding a Brand: A Classification Based on Correspondence Analysis. Communications in Dependability and Quality Management. 19(1), 5-17.

[15] Darabi-Golestan, F., Hezarkhani, A., 2018. Evaluation of elemental mineralization rank using fractal and multivariate techniques and improving the per-

formance by log-ratio transformation. Journal of Geochemical Exploration. 189, 11-24.

[16] Wang, C.H., 2016. A novel approach to conduct the importance-satisfaction analysis for acquiring typical user groups in business-intelligence systems. Computers in Human Behavior. 54, 673-681.

[17] Kumru, M., Bakac, M., 2003. R-mode factor analysis applied to the distribution of elements in soils from the Aydın basin, Turkey. Journal of Geochemical Exploration. 77(2), 81-91.

[18] Collins, S.V., Boyce, J.I., 2004. Discriminant Function Analysis of Spectral Gamma Data as a Tool for Regional Stratigraphic Correlation of Pleistocene Deposits. AGU Spring Meeting Abstracts. pp. H41D-06.

[19] Swoboda, M., Arlt, R., Gostilo, V., et al., 2005. Spectral gamma detectors for hand-held radioisotope identification devices (RIDs) for nuclear security applications. IEEE transactions on nuclear science. 52(6), 3111-3118.

[20] Wershofen, H., Arnold, D., 2005. Radionuclides in Ground-level Air in Braunschweig: Report of the PTB Trace Survey Station from 1998 to 2003, Physikalisch-Technische Bundesanstalt.

[21] Darabi-Golestan, F., Hezarkhani, A., Zare, M., 2017. Assessment of ^{226}Ra, ^{238}U, ^{232}Th, ^{137}Cs and ^{40}K activities from the northern coastline of Oman Sea (water and sediments). Marine Pollution Bulletin. 118(1), 197-205.

[22] Darabi-Golestan, F., Hezarkhani, A., 2020. Discrimination geochemical interaction effects on mineralization at the polymetallic Glojeh deposit, NW Iran by interative backward quadratic modeling. Acta Geochimica. 39(2), 236-254.

[23] Belkhiri, L., Narany, T.S., 2015. Using multivariate statistical analysis, geostatistical techniques and structural equation modeling to identify spatial variability of groundwater quality. Water Resources Management. 29(6), 2073-2089.

[24] Deutsch, J.L., Palmer, K., Deutsch, C.V., et al., 2016. Spatial Modeling of Geometallurgical Properties: Techniques and a Case Study. Natural Resources Research. 25(2), 161-181.

[25] Akbarpour, A., Gholami, N., Azizi, H., et al., 2013. Cluster and R-mode factor analyses on soil geochemical data of Masjed-Daghi exploration area, northwestern Iran. Arabian Journal of Geosciences. 6(9), 3397-3408.

[26] Bu, C.F., Zhang, P., Wang, C., et al., 2016. Spatial distribution of biological soil crusts on the slope of the Chinese Loess Plateau based on canonical correspondence analysis. Catena: An Interdisciplinary Journal of Soil. 137, 373-381.

[27] Carranza, E.J.M., 2009. Controls on mineral deposit occurrence inferred from analysis of their spatial pattern and spatial association with geological features. Ore Geology Reviews. 35(3), 383-400.

[28] Darabi-Golestan, F., Hezarkhani, A., 2019. Multivariate analysis of log-ratio transformed data and its priority in mining science: Porphyry and polymetallic vein deposits case studies. Bulletin of the Mineral Research and Exploration. 159(159), 185-200.

[29] Ji, H., Zeng, D., Shi, Y., et al., 2007. Semi-hierarchical correspondence cluster analysis and regional geochemical pattern recognition. Journal of Geochemical Exploration. 93(2), 109-119.

[30] Abdi, H., Valentin, D., 2007. Multiple correspondence analysis. Encyclopedia of measurement and statistics. pp. 651-657.

[31] Anekwe, U.L., Ibe, S.O., 2021. Natural Radioactivity in Some Borehole Water in Ogbia Local Government Area, Bayelsa State, Nigeria.

[32] UN Scientific Committee on the Effects of Atomic Radiation, 2000. Sources and effects of ionizing radiation. New York: United Nations Publications.

[33] Tsabaris, C., Eleftheriou, G., Kapsimalis, V., et al., 2007. Radioactivity levels of recent sediments in the Butrint Lagoon and the adjacent coast of Albania. Applied Radiation and Isotopes. 65(4), 445-453.

[34] Ravisankar, R., Chandramohan, J., Chandrasekaran, A., et al., 2015. Assessments of radioactivity concentration of natural radionuclides and radiological hazard indices in sediment samples from the East coast of Tamilnadu, India with statistical approach. Marine Pollution Bulletin. 97(1), 419-430.

[35] Al-Trabulsy, H., Khater, A., Habbani, F., 2011. Radioactivity levels and radiological hazard indices at the Saudi coastline of the Gulf of Aqaba. Radiation Physics and Chemistry. 80(3), 343-348.

[36] Amekudzie, A., Emi-Reynolds, G., Faanu, A., et al., 2011. Natural radioactivity concentrations and dose assessment in shore sediments along the coast of Greater Accra, Ghana. World Applied Sciences Journal. 13(11), 2338-2343.

[37] Dar, M.A., El Saman, M.I., 2012. The radiation hazards of some radio-elements in petroleum and phosphate regions along the Red Sea, Egypt. Proceeding of The Third International on Radiation Sciences and Applications. 5(2), 920.

[38] Darabi-Golestan, F., Hezarkhani, A., Zare, M.R., 2019. Geospatial analysis and assessment of ^{226}Ra, ^{235}U, ^{232}Th, ^{137}Cs, and ^{40}K at Anzali wetland, north of Iran. Environmental Monitoring and Assessment. 191(6), 1-15.